J Mater Sci (2008) 43:4915–4920
DOI 10.1007/s10853-008-2715-x

Effect of twin-boundaries on melting of aluminum

Sardar Sikandar Hayat · Muhammad A. Choudhry · Sheikh A. Ahmad

Received: 21 March 2008 / Accepted: 8 May 2008 / Published online: 30 May 2008

Abstract Molecular dynamics simulation technique has been applied to investigate melting temperature of aluminum. Semi-empirical potentials, based on the embedded atom method have been employed to calculate lattice parameter, energy per atom and mean square displacements. Melting temperature is found to compare well with the experimental results. Computer simulation studies of some low index (111), (113) and (112) twin boundaries at various temperatures and their effect on the melting temperature are also carried out. It is observed in this study that in the presence of twin boundaries, aluminum melts at lower temperatures, as compared to normal melting point.

Introduction

Pure aluminum is soft, ductile, and corrosion resistant and has a high electrical conductivity. The use of aluminum and its alloys in automotive industry has increased in recent years [1]. This has been attributed not only to the issue of fuel economy, but also to that of safety, resource conservation, and environment [2]. Presence of defects may change the properties of pure metal considerably. The effect of grain boundaries has been the subject of interest to material scientists [3–6].

Melting temperature (T_m) is an important parameter of a material as it indicates its stability against heating. The fundamental concept of melting is based on the coexistence of the solid with the liquid phase when the free energies of the two phases are equal. Different theories on melting have been proposed treating the phenomena as a homogenous, bulk process involving either lattice instability [7] or the spontaneous generation of thermal defects [8]. These descriptions do not consider effects of extrinsic defects such as a free surface or an internal interface. However, now a variety of experimental data exists which explains the controlling role of an extrinsic surface [9–13]. In several measurements it is clear that when the surface conditions are modified, the melting can be depressed [10] or the solid can be substantially superheated [12, 13]. In the case of metals, disordering below T_m on aluminum surface has been observed by Stoltze et al. [13]. Measurements have also been carried out to investigate the possibility of premelting transition [14, 15]. Static measurements of energy and structures of twin boundaries for f.c.c. metals are available in literature [16]. Premelting due to the internal interfaces, e.g., grain boundaries, can be realized through atomistic simulation using the method of molecular dynamics (MD) [17].

The MD and other related methods of Monte Carlo [18] have been successfully used to calculate phase diagrams of model systems [19] as well as to study melting and freezing phenomena [20]. These are powerful techniques for dealing with the statistical mechanics of a many-body system. Their applications to real materials have limitations imposed by the interatomic potential used and the finite system size and time duration of simulation. The advent of many-body potentials [21–23] for metals eliminates several basic objections against the use of conventional pair potential [24]. MD computer simulation method, based on many-body interatomic potentials, has become an established tool in materials science to evaluate many properties [25, 26]. By the use of this technique, one can investigate and understand structures of complex system at atomic

S. S. Hayat (✉) · M. A. Choudhry · S. A. Ahmad
Department of Physics, Islamia University of Bahawalpur, Bahawalpur, Punjab 63100, Pakistan
e-mail: sikandariub@yahoo.com

level and can follow the evolution of the system at each step. Another aspect of molecular dynamics relevant to the present study is the determination of the melting point T_m of the simulated model.

Embedded-Atom-Method (EAM) potentials [21, 27] have been developed for f.c.c. metals by fitting experimental parameters like lattice constants, cohesive energy, and vacancy formation energy. These potentials have produced very useful and reliable results [28]. Akhter et al. [29] employed EAM potential to study the three low index surfaces of Pd, namely (100), (110), and (111), by the MD technique. They have reported considerable premelting by measuring the mean square vibrational amplitudes and the structure factors. The potential with cut-off distance between the third and fourth nearest neighbor produced plausible results on melting temperature, specific heat, linear thermal coefficient, and diffusion coefficient of Pd [30]. Ahmed et al. [31] and Akhter et al. [32] have reported thermal properties of noble metals Ag and Au by MD simulations using EAM potential which reasonably agreed with the experimental results. The EAM potential has also been used to study grain boundaries in b.c.c. and f.c.c. metals [33–35]. Recently Park et al. [6] have studied the deformation of f.c.c. nanowires by twinning and slip using EAM potential.

In this paper, attention has been focused on melting temperature and the role of twin boundaries on melting of Al by means of MD simulations using an EAM potential function with interactions extending to third nearest neighbor distance. We have calculated the lattice parameter, energy per atom, and mean square displacement at various temperatures and deduced the melting temperature of the perfect crystal. Low index (111), (113), and (112) twin boundaries were generated and finally melting checked in the presence of these twin boundaries. The results are compared with available data in the literature.

Computational technique

We mainly followed '*dyn86*' molecular dynamics (MD) Foiles code containing DYNAMO routine. We introduced lattice and twin generating routines according to the requirement of the problem. The detailed MD technique can be found in literature [21, 27]. The salient features of the technique as applied in our case are given here. Nordsieck's algorithm [36] with a time step of 10^{-15} s was used to solve classical equations of motion for atoms interacting by EAM interatomic potential [21, 27]. The computational cell used consisted of 256 atoms arranged on an f.c.c. lattice. All simulations were carried out using periodic boundary conditions in the x, y, and z directions of the cubic simulation cell, and the cut-off distance was kept between the third and fourth nearest neighbor distance. Simulation was carried out in different statistical ensembles. We used the condition of constant number of atoms, pressure, and temperature (NPT) ensemble to calculate the lattice parameters at various temperatures. The computational cell was generated at a specific temperature while keeping the pressure constant; the system was allowed to evolve till the cell edges and volume become constant. The lattice constants thus obtained are used to generate the bulk f.c.c. crystal at various temperatures.

A discrete three-dimensional lattice model of a crystal with desired defect can be simulated by using results obtained by NPT ensemble below melting at various temperatures. The energy and atomic structure of this model is monitored along with all of its details. In order to study the twin boundaries, three-dimensional model crystallite generated is in the form of a rectangular block of atoms, with suitable mutually perpendicular axes. All the atoms in the computational region are free to move. The faces parallel to the interfaces are kept under fixed boundary conditions, while periodic boundary conditions are imposed on rest of the faces. The energy of the perfect crystal 'E_p' is first calculated, then a twin interface is introduced at the center of the computational cell. The energy of the crystal is again calculated '$E_p + \gamma$' (which is energy of the crystal with defects) using the condition of constant number of atoms, volume, and energy (NVE) ensemble simulations. The energy of the twin 'E_γ' can be calculated as

$$E_\gamma = E_{p+\gamma} - E_p$$

The crystal is first allowed to relax to minimize its energy by conjugate gradient method [37], and then relaxed energy of the twin is calculated.

Results and discussion

To calculate the lattice parameter at various temperatures we used NPT simulation. The computational cell is generated at a particular temperature and then keeping the pressure and temperature constant. The system is allowed to evolve till the cell edges and volume become constant. The lattice parameter is calculated from $a = (4\Omega)^{1/3}$, where Ω is the calculated average atomic volume at each temperature.

Melting temperature

The internal energy per atom '$E(T)$' was calculated as a function of temperature from 300 to 1,200 K using NPT simulation. Results are plotted in Fig. 1 which shows a sudden jump between 900 and 905 K. The data for the energy per atom is fitted to a third order polynomial in the

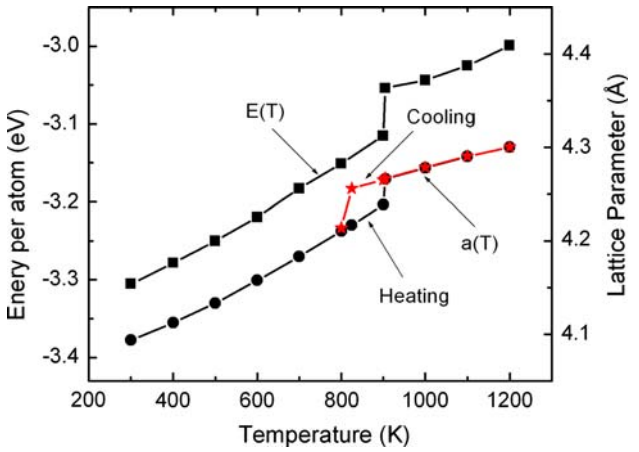

Fig. 1 Energy per atom (eV) and lattice parameter (Å) at various temperatures. A sudden change is seen in both curves at the same temperature 900 K, which is melting temperature of Al

temperature range 300–800 K below melting temperature as given in the following equation:

$$E(T) = E_0 + A_1\left(\frac{T}{T_m}\right) - A_2\left(\frac{T}{T_m}\right)^2 + A_3\left(\frac{T}{T_m}\right)^3$$

where '$E(T)$' is energy per atom at temperature 'T' in 'eV' and T_m = 900 K is the melting temperature obtained in the present study. The values of constants E_0, A_1, A_2, and A_3 are summarized in Table 1.

Calculated lattice parameter '$a(T)$' as a function of temperature is also shown in lower curve of Fig. 1. A sudden change in lattice parameter at same temperature indicates the transition from solid to liquid face where it was observed for energy per atom. The data for lattice parameter is also fitted to a third order polynomial in the temperature range below melting temperature (300–800 K) as given by the following equation:

$$a(T) = a_0 + B_1\left(\frac{T}{T_m}\right) + B_2\left(\frac{T}{T_m}\right)^2 - B_3\left(\frac{T}{T_m}\right)^3$$

The obtained values of constants a_0, B_1, B_2, and B_3 are also given in Table 1.

The energy per atom and the lattice parameter, plotted in the Fig. 1 as a function of temperature, clearly reveal a sudden jump between 900 and 905 K. Therefore it is concluded that the melting temperature of Al lies between 900 and 905 K. There is no superheating observed. When the system was cooled from higher temperature, the transition from liquid to solid state was observed between 825 and 800 K. This indicates the presence of supercooling.

Table 1 The constants of expressions for energy per atom and lattice parameters

Energy		Lattice parameter	
E_0	−3.50532	a_0	4.0608
A_1	0.76954	B_1	0.03901
A_2	0.77825	B_2	0.19811
A_3	0.40721	B_3	0.05879

The mean square displacements (MSD) of bulk atoms also give indication of the melting transition. At melting, these displacements increase enormously and the magnitudes become a few tenths of the interatomic distances [38]. The MSD values at different temperatures are calculated using the following equation:

$$\left\langle U_{ix}^2 \right\rangle = \frac{1}{N_j}\sum_{i=1}^{N_j}\left\langle \left[r_{ix}(t) - \left\langle r_{ix}(t-\tau)\right\rangle_\tau\right]^2\right\rangle$$

where 'r_{ix}' is the instantaneous position of atom i in the direction x and 'τ' is the time interval after which the configurations were recorded. The angular brackets $\langle\rangle$ denote the time average taken over all N_j recorded configurations. There is an abrupt jump in MSD at temperature 900 K, which is the melting temperature of the Al obtained from the energy per atom and lattice parameter as well. As the mean square displacements increase by the order of magnitude after melting, a log scale plot is given in Fig. 2. It is clear that mean square displacements increase linearly with temperature up to the point of transition and then there is a sharp increase in values.

We deduced that 900 K is the melting temperature of the Al obtained from the energy per atom, lattice parameter, and mean square displacements. Our result of 900 K melting temperature of Al agrees reasonably with the experimental value of 933 K [39] as compared to the value given by Mitev et al. [40], which is 980 K. This is an

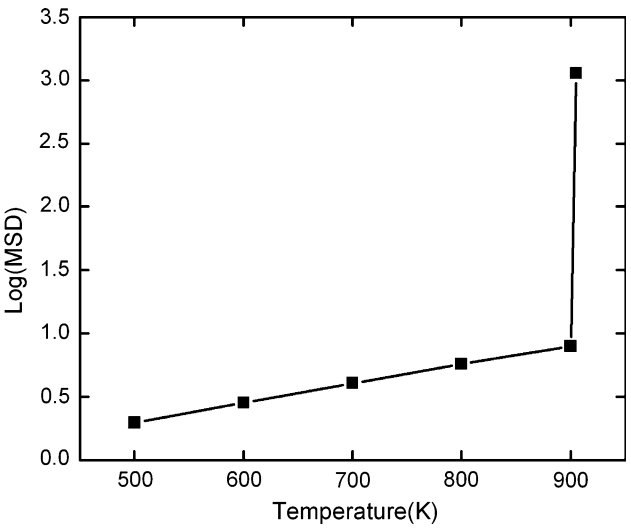

Fig. 2 Mean square displacement as a function of temperature. A sharp increase is observed in the value of mean square displacement at 900 K

excellent way for the judgment of the exact melting point of a material by observing the variation in lattice parameter, energy per atom, and mean square displacements.

Melting in the presence of twin boundaries

To study the effect of twin boundaries on melting we generated the model f.c.c. crystal consisting of a three-dimensional rectangular block of atoms. The twin boundary is located as close as possible to the center of the model. After generating a model twined crystal, atoms were allowed to relax from their initial approximate positions to their equilibrium configuration using conjugate gradient method. The size independency was achieved by the use of periodic boundaries in the calculation of twin formation energy. The crystallite developed for the (111) twin boundary is a rectangular block of atoms having faces $(11\bar{2})$, (111), and $(1\bar{1}0)$. The computational cell has $18(11\bar{2})$, 24(111), and $2(1\bar{1}0)$ planes. The (111) faces are kept fixed while the other faces are under periodic boundary conditions. The twin boundary is generated on the central plane of the model. The relaxed structure of (111) twin interface is shown in Fig. 3a. This fully relaxed (111) twin boundary has energy 84.53 mJ/m^2 at 0 K. The computational cell for (113) twin boundary consisted of $44(33\bar{2})$, 22(113), and $2(1\bar{1}0)$ planes. Rigid boundary conditions are applied on the faces parallel to (113) twin interface and cyclic periodic boundary conditions are applied on the faces perpendicular to the (113) twin interface. The twin boundary is generated at the middle (113) plane. The fully relaxed structure of (113) twin is shown in Fig. 3b which has energy 209.19 mJ/m^2 at 0 K.

The model crystal used to create a (112) twin boundary is a rectangular block of atoms with $24(11\bar{1})$, 18(112), and $2(1\bar{1}0)$ planes. The (112) faces are kept under rigid boundary conditions, whereas the other four faces are simulated with periodic boundary requirements. The twin is generated at the center of the model. In the unrelaxed structure of (112) twin, atoms in the plane adjacent to the composition plane lie at a separation of 0.2082a, which is nearly 58% of the first neighbor distance in perfect crystal. So one can expect a high energy for (112) twin interface. The fully relaxed structure of (112) twin is shown in Fig. 3c which has energy 500.28 mJ/m^2 at 0 K.

The (111), (113), and (112) twin interfaces are simulated in the temperature range 0–800 K, in steps of 100 K. The formation energies of these twin interfaces against temperature are plotted in Fig. 4. We observed that the (111) twin interface with high planer atomic density and greater interplanar spacing has low twin formation energy. The (112) twin interface with low planer atomic density and smaller interplanar spacing has high twin formation energy. The present results of twin interfaces are satisfactory in the sense that the atomic relaxations which occur are all consistent with what might be anticipated using hard sphere model. The relative energies which have been deduced are acceptable. The magnitudes of most of the twin formation energies are lower than the earlier simulated results of these interfaces, obtained by using Ackland many-body potential for other f.c.c. metals [16].

For observing the effect of twin interfaces on melting temperature, the internal energy per atom and lattice parameter are calculated as a function of temperature in the

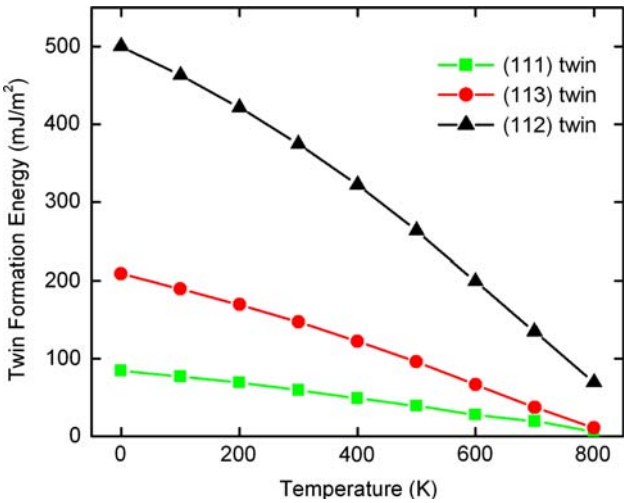

Fig. 4 The plot of twin formation energy (mJ/m^2) versus temperature (K) for (111), (113), and (112) twin boundaries. All the plot lines show that with the increase of temperature twin formation energy reduces

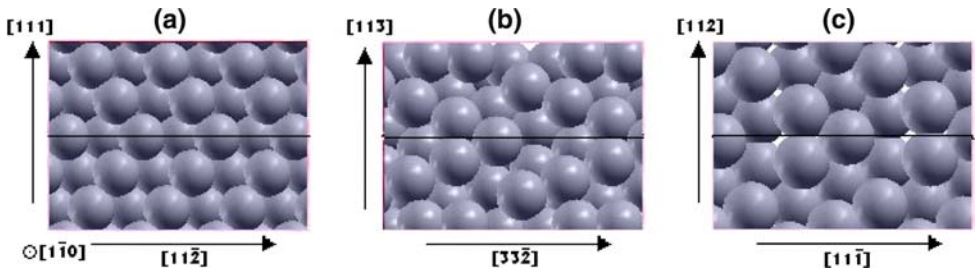

Fig. 3 Relaxed structure projected on $(1\bar{1}0)$ plane showing two adjacent layers of (**a**) (111) twin, (**b**) (113) twin, and (**c**) (112) twin boundary. Horizontal mid-lines show twin boundaries

range 300–1,100 K with 100 K steps using NPT simulation for (111), (113), and (112) twined crystallites. Results of energy per atom for (111) twined crystallite are plotted in Fig. 5a, which shows a sudden jump between 875 and 885 K. A plot of calculated lattice parameter as a function of temperature is also given in Fig. 5a. A transition can again be noted at the same temperature where it was observed for energy per atom. These transitions in lattice parameter and energy per atom curves confirmed that the melting point of the (111) twined crystallite is 875 K, which is 25 K lower, as compared to simulated normal melting point. Results of energy per atom and lattice parameter as a function of temperature for (113) twined crystallite are plotted in Fig. 5b, which shows a sudden jump between 850 and 860 K for both curves. Thus the melting point of the (113) twined crystallite is at 850 K, which is 50 K lower, as compared to normal melting point of the perfect crystal. Similarly, these transitions in lattice parameter and energy per atom are plotted in Fig. 5c for (112) twined crystallite. The jumps in curves are between 800 and 810 K. We estimated the melting point of the (112) twined crystallite to be 800 K, which is 100 K lower than normal simulated melting point.

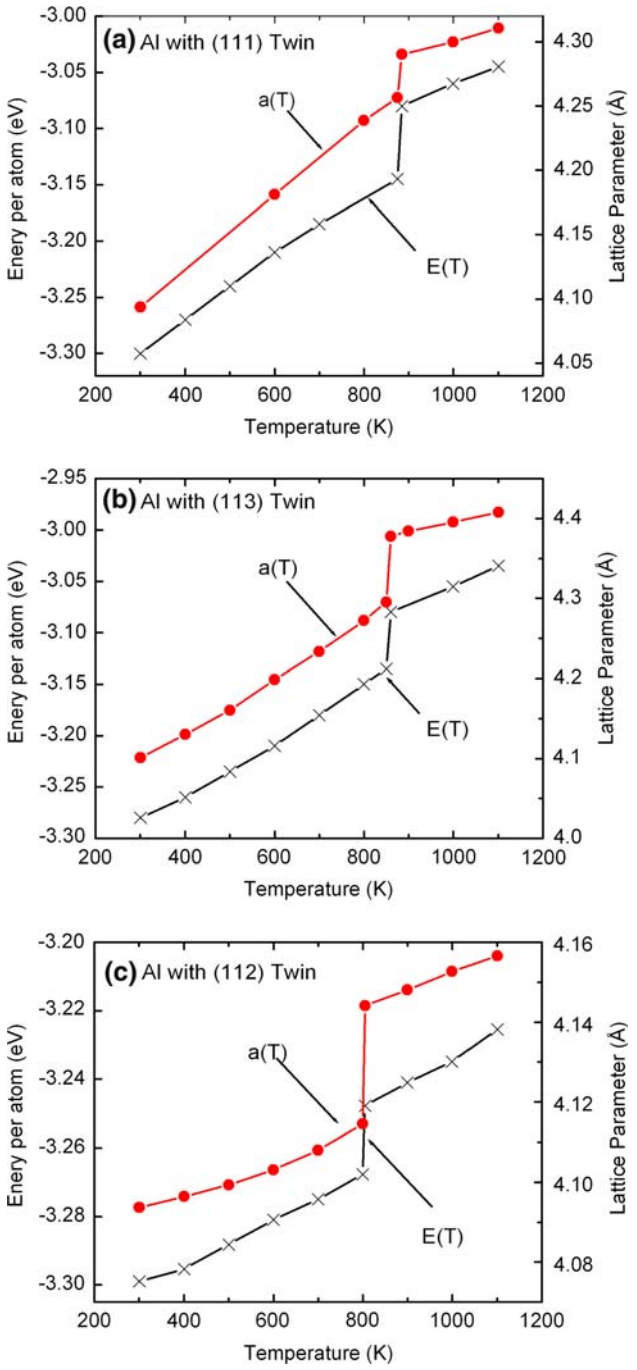

Fig. 5 Energy per atom (eV) and lattice parameter (Å) of Al (**a**) with (111) twin, (**b**) with (113) twin, and (**c**) with (112) twin at various temperatures

Atoms in the grain-boundary core have higher potential energy than that of the bulk atoms and it seems reasonable that the interface can become thermally disordered before the bulk or has its own melting transition. Indirect experimental evidence and theoretical considerations [41, 42] support such behavior. Near the twin boundaries atomic density is different as compare to normal plane. With the increase in temperature, the number of self interstitials and vacancies increases around the twin plane, thus the diffusion is likely to begin in crystal at the twin boundaries. At a sufficiently high temperature, in the vicinity of twin plane, the atoms are in complete disorder. This disordering and diffusion can lead to premelting near twin boundaries, which enhance the effect of melting process. Therefore the bulk crystal with twin boundaries melts at lower temperature than the normal melting point.

We observed that the transition from solid to liquid face takes place in the range of 10 K temperature for twined crystallite, while transition range was 5 K for perfect crystal. Transition temperature with defects increased. So we can say that there is superheating observed as compared to normal crystal. Thus sharpness of the melting point is reduced. Our calculations estimate $T_m(111) \cong 875 \pm 10$ K, $T_m(113) \cong 850 \pm 10$ K, and $T_m(112) \cong 800 \pm 10$ K for (111), (113), and (112) twined crystallites, respectively. We observed that there is smaller effect on melting temperature with (111) twin boundary and greater effect with (112) twin boundary. Sudden change in lattice parameter and energy per atom is used to investigate the melting point of metals. This was also used by Akhter et al. [30, 33] and Ahmed et al. [32]. The results presented in this paper can be relied upon as they have been obtained using a well-established suit of computer programs, which have already produced plausible results for other f.c.c. metals [30–33].

Conclusions

In this study, melting temperature was computed in three different ways, i.e., by looking at variation in lattice parameter, energy per atom, and mean square displacements as a function of temperature. Our calculations estimate $T_m \cong 900 \pm 5$ K for defect-free Al crystal. This value is more close to the experimental value of 933 K [39] as compared to the value recently simulated by Mitev et al. [40], which is 980 K.

The EAM potential is also employed to study some low index (111), (113), and (112) twin boundaries. The calculated twin formation energies are 84.53, 209.19, and 500.28 mJ/m^2 for (111), (113), and (112) twins, respectively, at 0 K. These energies decrease with the increase of temperature. These energies approach 6.25, 10.86, and 69.37 mJ/m^2 for (111), (113), and (112) twin boundaries, respectively, at 800 K. We observed that crystallite melts at 875 K with (111) twin interface, at 850 K with (113) twin interface and at 800 K with (112) twin interface. The interplanar spacing of (111), (113), and (112) planes are 0.5773a, 0.3015a, and 0.2041a, respectively. We concluded that

(i) The (111) twin interface with high planer atomic density and greater interplanar spacing shows smaller decrease in melting temperature (25 K)
(ii) The (112) twin interface with low planer atomic density and smaller interplanar spacing shows greater decrease in melting temperature (100 K)
(iii) Sharpness of melting point reduces in twined crystals, thus some superheating appears.

Acknowledgements The work of S.S.H. and M.A.C. was supported by the Higher Education Commission (HEC) of Pakistan. We are indebted for useful discussion to J. I. Akhter of Physics Division, PINSTECH, Pakistan.

References

1. Aluminum Autodesign Review (1998) Aluminum Soc 6(3):1
2. Aluminum Standards and Data (1990) The aluminum association. Washington, DC
3. Tang M, Carter WC, Cannon RM (2006) J Mater Sci 41:7691. doi:10.1007/s10853-006-0608-4
4. Jian-Min Z, Yu-Hong H, Ke-Wei X, Vincent J (2007) Chinese Phys 16:210. doi:10.1088/1009-1963/16/1/036
5. Pollet L, Boninsegni M, Kuklov AB, Prokof'ev NV, Svistunov BV, Troyer M (2007) Phys Rev Lett 98:135301. doi:10.1103/PhysRevLett.98.135301
6. Park HS, Gall K, Zimmerman JA (2006) Mech Phys Solids 54:1862. doi:10.1016/j.jmps.2006.03.006
7. Boyer LL (1985) Phase Transit 5:1. doi:10.1080/01411598508219144
8. Cahn RW (1978) Nature 273:491. doi:10.1038/273491b0
9. Cahn RW (1986) Nature 323:668. doi:10.1038/323668a0
10. Boyce JB, Stutzmann M (1985) Phys Rev Lett 54:562. doi:10.1103/PhysRevLett.54.562
11. Rossouw CJ, Donnelly SE (1985) Phys Rev Lett 55:2960. doi:10.1103/PhysRevLett.55.2960
12. Daeges J, Gleiter H, Perepezko JH (1986) Phys Rev Lett 119:79
13. Stoltze P, Norskov JK, Landman U (1988) Phys Rev Lett 61:440. doi:10.1103/PhysRevLett.61.440
14. Chan SW, Liu JL, Balluffi RW (1985) Scr Metall 19:1251. doi:10.1016/0036-9748(85)90248-0
15. Balluffi RW, Maurer R (1988) Scr Metall 22:709. doi:10.1016/S0036-9748(88)80187-X
16. Faridi BAS, Ahmad SA, Choudhry MA (1991) Ind J Pure Appl Phys 29:796
17. Ciccotti G, Frenkel D, McDonald IR (1987) Simulations of liquids and solids. North Holland, Amsterdam
18. Binder K (ed) (1979) Monte Carlo methods in statistical physics. Springer-Verlag, Berlin
19. Broughton JQ, Li XP (1987) Phys Rev B 35:9120. doi:10.1103/PhysRevB.35.9120
20. Nose S, Yonezawa F (1985) Sol Stat Comm 56:1009; (1986) J Chem Phys 84:1803. doi:10.1063/1.450427
21. Daw MS, Baskes MI (1984) Phys Rev B 29:6443. doi:10.1103/PhysRevB.29.6443
22. Finnis MW, Sinclair JE (1984) Philos Mag A 50:45. doi:10.1080/01418618408244210
23. Manninen M (1986) Phys Rev B 34:8486. doi:10.1103/PhysRevB.34.8486
24. Oh DJ, Johnson RA (1988) J Mater Res 3:471. doi:10.1557/JMR.1988.0471
25. Michael JM, Dimitrios AP (1996) Phys Rev B 54:4519. doi:10.1103/PhysRevB.54.4519
26. Cagin T, Dereli G, Uludogan M, Tomak M (1999) Phys Rev B 59:3468. doi:10.1103/PhysRevB.59.3468
27. Foiles SM, Baskes MI, Daw MS (1986) Phys Rev B 33:7983. doi:10.1103/PhysRevB.33.7983
28. Mei J, Davenport JW (1990) Phys Rev B 42:9682. doi:10.1103/PhysRevB.42.9682
29. Akhter JI, Yaldram K, Ahmad W (1996) Sol Stat Comm 98:1043. doi:10.1016/0038-1098(96)00137-8
30. Akhter JI, Yaldram K (1997) Int J Mod Phys C 8:1217. doi:10.1142/S0129183197001089
31. Ahmed E, Akhter JI, Ahmad M (2004) Comput Mater Sci 31:309
32. Akhter JI, Ahmed E, Ahmad M (2005) Mater Chem Phys 93:504. doi:10.1016/j.matchemphys.2005.03.048
33. Lutsko JF, Wolf D, Phillpot SR, Yip S (1989) Phys Rev B 40:2841. doi:10.1103/PhysRevB.40.2841
34. Wolf D, Lutsko JF (1988) Phys Rev Lett 60:1170. doi:10.1103/PhysRevLett.60.1170
35. Lutsko JF, Wolf D (1989) Scr Metall 22:1923. doi:10.1016/S0036-9748(88)80239-4
36. Nordsieck A (1962) Math Comput 16:22. doi:10.2307/2003809
37. Fletcher R (1972) A FORTRAN subroutine for minimization by the method of conjugate gradients, AERE-R7073
38. Ubbelohde AR (1978) The Molten State of matter (Melting and crystal structure). Wiley, New York
39. Ashcroft NW, Mermin ND (1976) Solid state physics. Holt, Rinehart, Winston, New York
40. Mitev P, Evangelakis GA, Kaxiras E (2006) Model Simul Mater Sci Eng 14:721. doi:10.1088/0965-0393/14/4/013
41. Nguyen T, Ho PS, Kwok T, Yip S (1986) Phys Rev Lett 57:1919
42. Hart EW (1972) In: Hu H (ed) The nature and behavior of grain boundaries. Plenum, New York, p 155